BEEDLE: A Microneedle-Based Implant for Targeted Neurorestorative Therapy in Traumatic Brain Injury and Neurodegenerative Disorders

Damaris Kola-Asa and Youlan Li
Independent Researchers

Abstract

Traumatic brain injury (TBI) and neurodegenerative disorders—including stroke, Parkinson's disease, and Alzheimer's disease—present significant therapeutic challenges due to their complex pathology and the limitations of current drug delivery systems. A major obstacle is the blood-brain barrier (BBB), which restricts the passage of brain-healing compounds (neurorestorative agents), reducing their therapeutic potential. This paper introduces the Brain-Enhancing Embedded Device with Localized Efficiency (BEEDLE), a microneedle-based implant designed to overcome these limitations by enabling precise, sustained drug delivery to brain regions that support regeneration, such as the hippocampus and subventricular zone (neurogenic niches). BEEDLE bypasses the BBB, allowing direct administration of nerve growth–promoting molecules (neurotrophic factors), anti-aging cell-clearing drugs (senolytic agents), and neurotransmitter regulators (stabilizers) to promote the growth of new neurons (neurogenesis), strengthening of neural connections (synaptic plasticity), and the formation of new blood vessels (angiogenesis). BEEDLE uses a phased-release mechanism featuring a rotating drug cartridge and microcontroller-regulated dosing to optimize outcomes while minimizing side effects.

Preliminary validation through mechanical simulations confirms accurate drug targeting, with microneedle penetration and displacement tests showing minimal tissue damage. Computational models further support BEEDLE's ability to control drug spread over time (time-dependent diffusion), highlighting its promise for precisely targeted brain repair. This study evaluates BEEDLE's potential to transform treatment for TBI and other neurodegenerative diseases. By focusing drug delivery at the source of damage (localized biochemical intervention), BEEDLE offers a powerful alternative to traditional whole-body (systemic) treatments and current brain stimulation methods (neuromodulation). Future versions will aim to miniaturize the device, enhance drug packaging methods (encapsulation), and integrate biosensors

for real-time adaptive dosing. Combining biomedical engineering, neuropharmacology, and electronic control, BEEDLE represents a scalable and customizable advance in long-term brain repair (neurorehabilitation).

1. Introduction

Traumatic brain injuries (TBIs) affect nearly 49 million people worldwide, with treatment costs ranging from $85,000 to $3 million per patient (Guan et al., 2023; Egenberg Trial Lawyers, 2022). TBIs result in both primary mechanical injury and secondary neurodegeneration, the latter involving cellular senescence, chronic neuroinflammation, oxidative stress, and apoptosis (Sahel et al., 2019; Shao et al., 2022; Ng & Lee, 2019; Wu et al., 2022). The primary phase of TBIs occurs at the moment of impact, causing immediate damage to brain tissue through direct force application, rotational acceleration, or rapid deceleration. This mechanical disruption leads to the shearing of axons, vascular damage, immediate neuronal destruction, synaptic dysfunction, and metabolic disturbances that set the stage for secondary injuries (Logsdon et al., 2015; Hoffe & Holahan, 2022; Srihagulang et al., 2021). The secondary phase of neuronal injury, occurring over hours to weeks after an initial insult, involves molecular and cellular cascades that exacerbate neuronal loss. Persistent neuroinflammation, mitochondrial dysfunction, and epigenetic modifications contribute to this process. Targeting pathways such as CX3CR1 modulation, mitochondrial protection, and HDAC2 inhibition have shown the potential to mitigate neurodegeneration and enhance recovery (Ertürk et al., 2016; Davidson et al., 2021; Lin et al., 2017). Additionally, MMP-9 inhibition may reduce BBB disruption and improve outcomes (Hadass et al., 2013). However, delivering these therapeutics effectively remains a challenge.

A major limitation in neurorestorative treatment is crossing the highly selective blood-brain barrier (BBB), which blocks 95% of therapeutic molecules from entering the brain (Achar et al., 2021; Dong, 2018). The BBB, composed of specialized endothelial cells with tight junctions, restricts paracellular permeability and blocks neurotoxic components, blood cells, and pathogens (Ayloo & Gu, 2019; Sweeney et al., 2019). It maintains homeostasis through selective molecular transport via carriers, ion channels, and receptor-mediated transcytosis, while low vesicle trafficking minimizes non-specific transcytosis, preserving barrier integrity (Ayloo & Gu, 2019; Saunders et al., 2016). However, this protective function of BBB also impedes the delivery of many potentially beneficial drugs, including neurotrophic factors, anti-inflammatory agents, and senolytic compounds (Patel & Patel, 2017). Existing solutions, such as deep brain stimulation (DBS), vagus nerve stimulation (VNS), and systemic drug delivery, offer symptom management rather than true

neuroregeneration (Xu et al., 2024; Neren et al., 2016; Haneef & Skrehot, 2023). Recent research has explored nanoparticle-based drug carriers, receptor-ligand conjugates, and ultrasound-mediated permeability modulation to enhance drug penetration, but these approaches remain limited in precision and long-term efficacy (Li et al., 2021).
Despite these advancements, no single existing technology effectively combines precise, localized drug delivery with long-term therapeutic control (Vora et al., 2020).

To address these challenges, we developed BEEDLE (Brain-Enhancing Embedded Device with Localized Efficiency), a microneedle-based implantable device for precise, localized neurorestorative therapy. Unlike systemic drug delivery, BEEDLE's phased-release mechanism administers neurotrophic factors, senolytic agents, and neurotransmitter stabilizers directly into neurogenic regions such as the hippocampus and subventricular zone (SVZ). By bypassing the BBB, BEEDLE enables sustained, controlled drug release while minimizing systemic side effects. The device incorporates an advanced microneedle array that allows direct drug administration into neurogenic niches, ensuring targeted intervention. Its automated cartridge system regulates phased drug delivery over extended periods, enhancing therapeutic control. Furthermore, the modular nature of BEEDLE enables customization for different neurodegenerative conditions, making it adaptable beyond TBI treatment. Its minimally invasive design reduces the need for repeated interventions, offering a patient-friendly alternative to conventional neuromodulation therapies. However, as with any implantable brain device, ethical considerations—such as long-term safety, equitable access, and the risk of cognitive or behavioral modulation—must be carefully addressed through preclinical testing and transparent regulation.

Neurogenesis, the process of generating new neurons, occurs primarily in two key regions: the hippocampus and the subventricular zone (SVZ) (Ming & Song, 2011). These regions are critical for cognitive function, neuroplasticity, and the brain's ability to recover from neurological conditions (Dennis et al., 2016). Within the hippocampus, the subgranular zone (SGZ) of the dentate gyrus serves as a key neurogenic niche. Neurogenesis in this region is closely associated with learning, memory formation, and stress recovery (Montalbán-Loro et al., 2021). Located along the lateral ventricles, the SVZ is another highly neurogenic region, continuously generating new neurons that migrate to the olfactory bulb and potentially other brain regions (Shabani et al., 2020). This process is regulated by a complex microenvironment of neural stem cells, astrocytes, and vascular components, which modulate neurogenic capacity (Platel & Bordey, 2016). Neurogenesis is regulated by both intracellular and extracellular signals, including nicotinic acetylcholine receptors, cytokines, and extracellular vesicles, which influence stem cell

differentiation and integration into neuronal circuits (Shabani et al., 2020). However, neurogenesis capacity declines significantly with age, limiting the brain's ability to self-repair (Miranda et al., 2019).

BEEDLE is designed to enhance neurogenesis by delivering key neuroregenerative compounds, including MFG-E8 (Milk Fat Globule-EGF Factor 8), brain-derived neurotrophic factor (BDNF), and Ginsenoside Rg1. MFG-E8 promotes neurogenesis by stimulating neural stem cell migration and differentiation via integrin αvβ3/αvβ5 (alpha-v beta-3 and alpha-v beta-5 signaling) signaling, which is crucial for restoring impaired neurogenesis in neurodegenerative diseases like Alzheimer's disease and Parkinson's disease (Cheyuo et al., 2019). Additionally, it reduces neuroinflammation by enhancing the phagocytic clearance of apoptotic neurons and supports vascular repair by promoting VEGF-dependent neovascularization, improving cerebral blood flow and neuronal survival (Silvestre et al., 2005). MFG-E8 also provides neuroprotection by reducing neuronal apoptosis through the integrin β3/FAK/PI3K/AKT (Integrin beta-3/Focal Adhesion Kinase/Phosphoinositide 3-Kinase/Threonine Kinase) signaling pathway. This mechanism is particularly beneficial following traumatic brain injury, as it decreases brain edema and improves neurological outcomes (Gao et al., 2018).

Similarly, brain-derived neurotrophic factor (BDNF) enhances neurogenesis by promoting neural stem cell proliferation and differentiation via TrkB signaling, while strengthening synaptic plasticity by supporting dendritic growth and neurotransmitter regulation (Numakawa & Kajihara, 2023). BDNF enhances synaptic plasticity by modulating synaptic transmission and long-term potentiation (LTP), particularly in the hippocampus (Leal et al., 2014). This is achieved through the activation of TrkB receptors, which influence protein synthesis and synaptic proteome regulation (Yamada & Nabeshima, 2003). The BDNF/TrkB signaling pathway is a potential target for therapeutic strategies aimed at mitigating cognitive decline and neurodegenerative diseases. Another Ginsenoside Rg1 contributes to neuronal protection by shielding against apoptosis and oxidative stress by modulating pathways such as Nrf2/ARE and Wnt/GSK-3β/β-catenin, enhancing antioxidant defenses, reducing inflammation, and aiding in cognitive functions such as learning and memory (Chu et al., 2018; Shi et al., 2010). Furthermore, these compounds initiate angiogenesis by activating the VEGF pathway, stimulating new blood vessel formation, improving circulation, and enhancing oxygen and nutrient delivery to neurons (Chen et al., 2019). Collectively, these biochemical therapies create a neurogenic, angiogenic, and neuroprotective environment, facilitating brain recovery and improving cognitive outcomes in traumatic brain injury (TBI) and neurodegenerative disorders.

Beyond TBI, BEEDLE's therapeutic potential extends to a range of neurodegenerative and mood disorders, including Alzheimer's disease,

Parkinson's disease, stroke, and depression. These conditions share overlapping genetic and molecular mechanisms, including chronic neuroinflammation, dopaminergic dysfunction, and neuronal loss (Tanaka et al., 2020; Reynolds et al., 2022; Ruffini et al., 2020). Existing treatments focus on symptom management rather than reversing neurodegeneration, leaving patients with limited long-term recovery options (Galts et al., 2019; De Marchi et al., 2023; Tan et al., 2019). BEEDLE addresses this gap by targeting disease-specific pathways to promote neuronal survival and synaptic repair.

While BEEDLE presents a promising approach for multiple neurological conditions, its initial implementation focuses on traumatic brain injury (TBI) patients under the age of 65, particularly within the Canadian healthcare system. This population was selected due to the high incidence of TBI in Canada—estimated at 165,000 new cases annually (Parachute Canada, 2022)—and the steep decline in neurogenesis capacity with age, which limits the effectiveness of regenerative therapies in older adults (Miranda et al., 2019). Canada's publicly funded, universally accessible healthcare system supports equitable deployment of advanced technologies like BEEDLE by reducing cost barriers and centralizing long-term care (Rowe, 2023). Moreover, Canada's national data infrastructure and post-acute rehabilitation network offer a strong foundation for early-stage trials and longitudinal tracking.

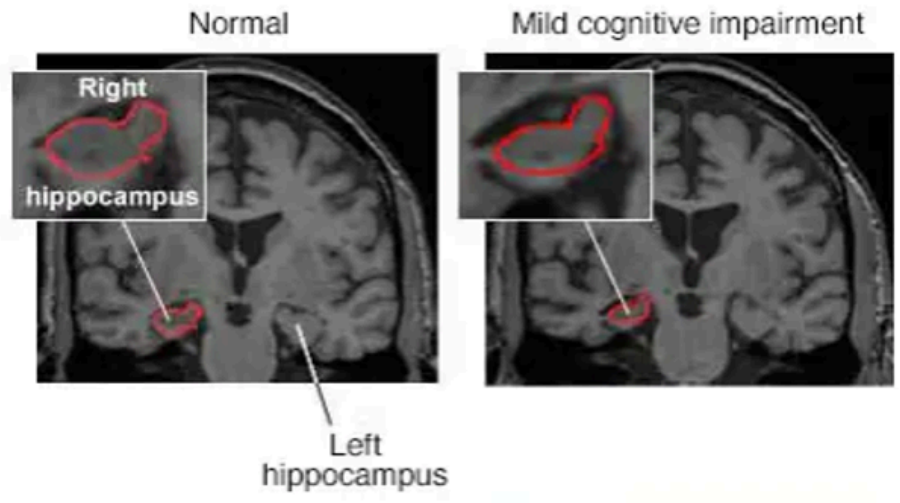

FIGURE 1. Hippocampal Shrinkage Revealed by MRI Scan (Mayo Clinic, n.d.)

By focusing on younger TBI patients in a system optimized for innovation and accessibility, BEEDLE maximizes its neuroregenerative potential, improving functional recovery and cognitive outcomes. While this study emphasizes Canadian feasibility, BEEDLE's modular design

and automated dosing system can be adapted to other healthcare contexts. Its scalable format may support integration into diverse care models, including insurance-based systems in the U.S. and hybrid public-private systems globally. This ensures that findings from Canadian implementation may serve as a blueprint for broader adoption. Although initially developed for TBI, BEEDLE's customizability allows expansion to other neurodegenerative conditions, such as Alzheimer's disease, Parkinson's disease, and stroke recovery—reinforcing its long-term relevance in global neurorehabilitation strategies.

Given the multifaceted challenges associated with TBI-induced neurodegeneration, an effective therapeutic approach must address both cellular dysfunction and drug delivery limitations. BEEDLE represents a novel intersection of biomedical engineering, neuropharmacology, and electronic control, offering a scalable and customizable neurorestorative solution. This paper will evaluate BEEDLE's design, including its automated drug-release mechanism, microneedle penetration accuracy, and phased drug diffusion. It will also assess BEEDLE's impact on neurological recovery, particularly in TBI, stroke, Parkinson's, and Alzheimer's disease. Additionally, this study will compare BEEDLE with existing neuromodulation techniques and traditional drug delivery methods while exploring future directions such as miniaturization, biosensor integration, and advanced drug stabilization strategies. By bridging biochemical neuroregeneration with precision engineering, BEEDLE has the potential to revolutionize neurorestorative medicine, transforming how TBI and neurodegenerative disorders are treated.

2. Methodology

2.1 Preparation and Setup

2.1.1 Brain Model Setup

To construct the simulated brain model for microneedle penetration testing, 800 (± 10) mL of gelatin mixture was prepared and poured into a brain-shaped silicone mold. The gelatin was left to set for 24 hours at 4 (± 1)°C to maintain structural integrity and prevent premature degradation. The mold dimensions, 24.89 cm ⊠ 17.78 cm ⊠ 8.13 cm, were selected to mimic realistic brain proportions, ensuring proper interaction with BEEDLE's microneedle array. This was replicated five times for five trials.

2.1.2 Head Model Setup

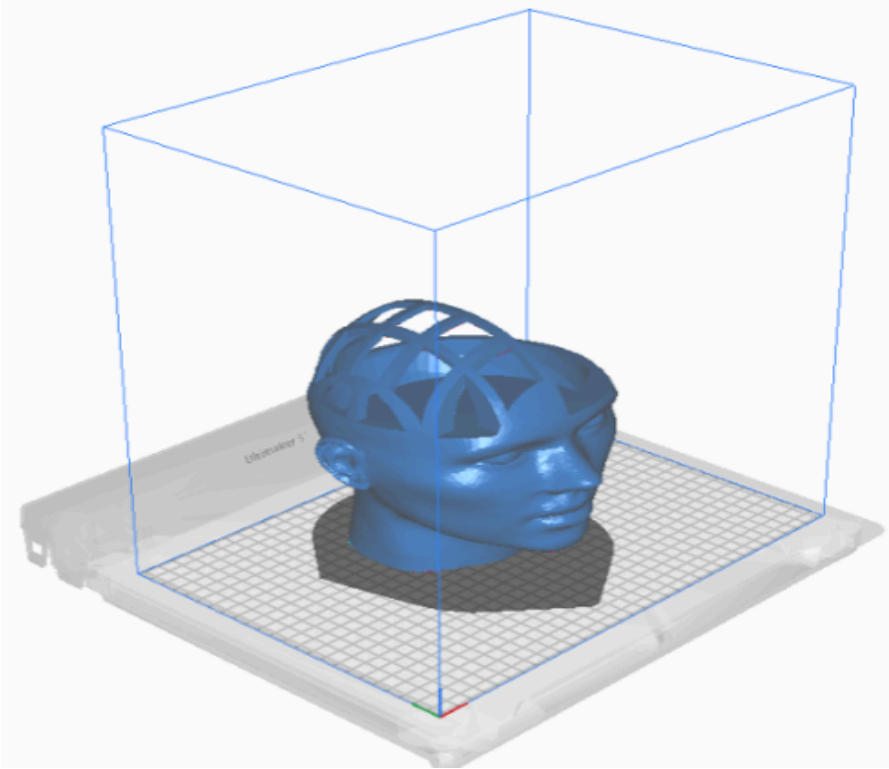

A 300 mm tall, 240 mm wide, and 225 mm deep, 3D-printed head model (Figure 2) was fabricated over 1 day, 8 hours, and 40 minutes to provide a structured multi-layered framework simulating the composition of a human head. The left hemisphere of the model featured a grid system with cranial fenestrations, which served as attachment points for securing the layered tissue components, while the right hemisphere contained a cavity to accommodate the gelatin brain model. A flat surface positioned at eye level was incorporated at the center to serve as a stable base for securing the gelatin model during trials.

The simulated head model was designed to replicate the biomechanical properties of the scalp, skull, and underlying brain tissue, incorporating four distinct layers to mimic anatomical structures. The outermost layer consisted of a 1 mm thick artificial epidermis, which was cut to conform to the curvature of the 3D-printed head and securely attached as the topmost layer. Beneath this, a 2 mm thick ballistic gel layer was prepared by dissolving the material in hot water per manufacturer instructions and pouring it into a shallow mold to replicate connective tissue. The third layer, representing the aponeurosis and pericranium, was constructed using 1.5 mm thick neoprene sheets and foam rubber, precisely cut to match the previous layers and simulate the structural support between the skin and

skull. The innermost component consisted of the high-density gelatin brain model, which was positioned within the cranial cavity of the 3D-printed head model. While this multi-layer structure approximates key mechanical barriers, it does not fully replicate the complex viscoelasticity, vascularity, or cellular heterogeneity of living tissue, and results should therefore be interpreted as preliminary approximations rather than direct biological analogs.

To ensure secure integration, holes were cut into each layer to align with the cranial fenestrations in the left hemisphere of the 3D-printed head model. Each layer was taped and bonded to these openings using medical-grade adhesive, ensuring that each simulated tissue layer was directly affixed to the head structure.

2.1.3 BEEDLE Assembly and Integration

The BEEDLE device is an automated microneedle-based drug delivery system designed to administer precise doses of medication over a controlled time frame. The device integrates a modular cartridge system, a servo-actuated plunger, and a rotational dispensing mechanism to ensure sequential, metered drug release through a microneedle array.

2.1.3.1 Structural Design

The core components of BEEDLE were manufactured using biocompatible materials, ensuring mechanical stability and safe interaction with pharmaceutical formulations. The device's modular construction enables scalability for different therapeutic applications. The microneedle array features uniformly spaced needles optimized for consistent drug diffusion, minimizing backflow and ensuring controlled absorption rates.

2.1.3.2 Electronic Integration and Control System

BEEDLE's microcontroller-based architecture governs its actuation sequence, ensuring precise timing, dosage consistency, and adaptability to user-defined treatment regimens. The system incorporates a servo-driven plunger that regulates medication flow rate based on preprogrammed dosing intervals, allowing for customized administration schedules. A rotational indexing mechanism advances the cartridge holder at designated time points, facilitating sequential drug release without external intervention. To enhance reliability, the system includes user interaction safeguards, such as debounce logic to prevent unintended activation or disruptions during operation. This flexible control structure enables BEEDLE to support a range of dosing protocols, making it adaptable for various neurotherapeutic applications.

Upon startup, the system initializes servo positions to eliminate mechanical drift, ensuring repeatable performance. BEEDLE's programmable dispensing intervals allow for flexible dosing regimens.

The microcontroller tracks elapsed time and automatically triggers sequential release, following an optimized time progression. This ensures scalable administration, adaptable for different pharmacokinetics and patient needs.

2.1.3.3 Actuation and Motion Control

To regulate drug flow, the plunger servo dynamically adjusts based on elapsed time, ensuring gradual and controlled release. At each dosing interval, the cartridge holder rotates to align the next reservoir with the microneedle array. This mechanical sequencing ensures high-precision dosing without requiring external intervention.

2.1.3.4 Power and System Redundancy

BEEDLE is powered by an integrated energy system with built-in failover protection, ensuring continuous operation in case of power fluctuations. The system employs modular battery integration, allowing for extended runtime and safe failure handling.

2.1.3.5 Diagnostics and Debugging

To enhance system reliability, BEEDLE includes real-time feedback mechanisms that log status updates during operation. These logs provide instantaneous system monitoring, facilitating troubleshooting and iterative optimizations.

2.1.4 Microneedle Penetration and Attachment to the Head Model

For each of the five trials, BEEDLE was pushed through all layers of the simulated head model, ensuring complete penetration through the outer skin, connective tissue, structural layers, and brain tissue. The microneedles advanced until they reached the hippocampus and subventricular zone (SVZ) within the gelatin brain model, ensuring the device delivered medication to the correct depth. The device was secured in place using double-sided tape, affixed to the exterior of the 3D-printed head, preventing movement during the test.

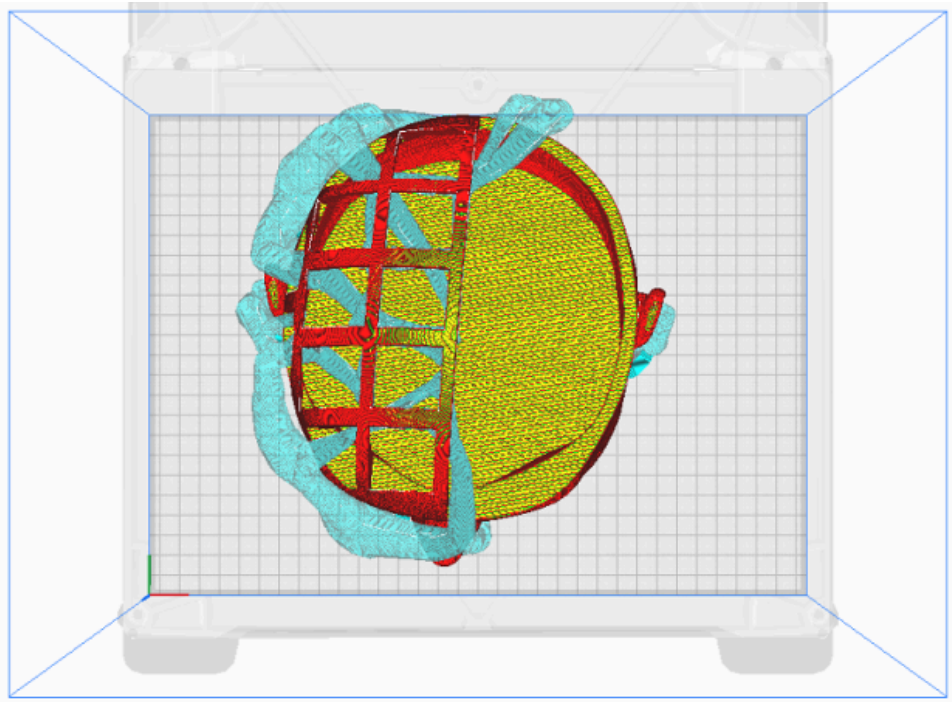

2.1.5 Dye Administration and BEEDLE Functionality Testing

Once BEEDLE was fully inserted, the start button was pressed, activating the automated drug delivery cycle. The system sequentially dispensed four cartridges, each containing 15.00 (± 0.01) mL of glycerin mixed with a distinct dye color, with a one-second delay between each activation. Cartridge 1 (Red dye) was dispensed for 1 minute, starting at t = 0 min. After a one-second delay, Cartridge 2 (Green dye) activated at t = 1 min 1 sec, releasing its contents over 5 minutes. Following another one-second delay, Cartridge 3 (Blue dye) was dispensed for 10 minutes, beginning at t = 6 min 2 sec. Finally, after an additional one-second delay, Cartridge 4 (Purple dye) began at t = 16 min 3 sec, delivering its payload over 20 minutes.

Glycerin was selected as a stand-in for neurorestorative compounds such as BDNF, MFG-E8, and Ginsenoside Rg1 due to its consistent viscosity, optical traceability, and ease of handling. While it offers a practical approximation for validating flow rate and timing within the microneedle system, glycerin does not fully replicate the molecular characteristics or diffusion behavior of the intended therapeutic agents. Consequently, future testing will incorporate compound-specific simulants to more accurately model delivery dynamics.

Throughout the cycle, the servo-controlled plunger ensured consistent dispensing, while the rotation servo automatically advanced the cartridge holder upon completion of each phase. After the final release at t = 36 min 4 sec, BEEDLE halted operation, and the microneedle array was carefully

withdrawn from the gelatin model. This sequence was repeated across five trials, with any inconsistencies in timing or volume of release recorded for further analysis.

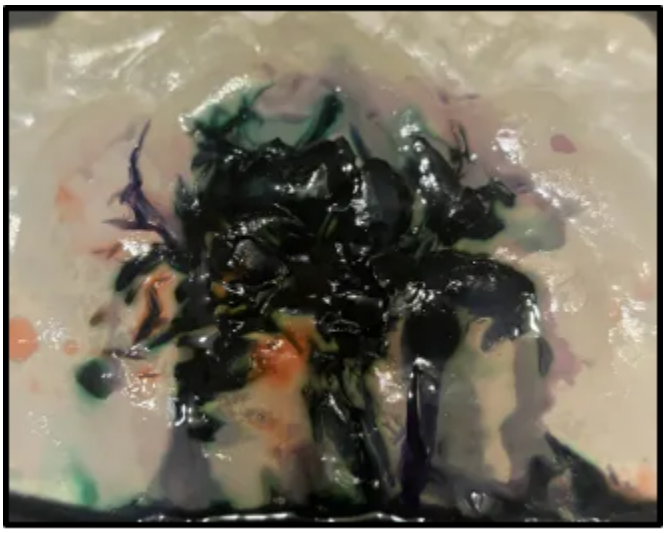

2.1.6 Functional Testing of BEEDLE

To validate BEEDLE's performance across five trials, four key tests were conducted to ensure precision, stability, and accuracy, with each measurement incorporating device-specific uncertainties. The Microneedle Penetration Test measured insertion depth using a digital caliper (±0.01 mm accuracy) to confirm that deviations remained within ±0.50 mm, accounting for both measurement uncertainty and mechanical tolerances. The Lateral Displacement Test assessed unintended sideways movement by comparing pre- and post-insertion reference points on a grid, with displacement visualized through a cross-section of the BEEDLE attachment site. Given the ±0.50 mm tolerance, this test ensured that lateral deviations were within acceptable limits for controlled insertion.

The Timing Verification Test recorded cartridge activation timestamps with a ±0.01 s precision to confirm dispensing at 1 min, 5 min, 10 min, and 20 min, with an operational tolerance of ±0.50 s to account for mechanical and electronic signal variations. Lastly, the Drug Delivery Volume Accuracy Test measured the gelatin brain model's weight before and after administration using a digital scale (±0.01 g accuracy) to verify precise dye release. Given the ±15.00 mL tolerance range, this test accounted for experimental inconsistencies such as expulsion, pooling, and microneedle retention. Results across all tests were averaged across trials to assess BEEDLE's reliability and precision in neurotherapeutic delivery.

2.1.7 Measurement and Data Collection

Each test was evaluated based on pass/fail criteria and quantitative measurements across all five trials. The average penetration depth, lateral displacement, and timing deviation were computed to assess BEEDLE's overall precision and reliability.

2.2 Materials

2.2.1 Device Materials

The following components were selected to ensure structural integrity, functional integration, and automated operation:

Structural Framework: Fabricated using high-durability, biocompatible materials optimized for stability and modularity.
Power System: Includes a primary rechargeable energy unit with an auxiliary backup power source to ensure continuous operation.
Control System: A microcontroller-driven actuation system manages automated dispensing and sequencing.
Actuation Mechanism: Utilizes a multi-phase motion control system to regulate targeted release and cartridge transitions.
User Interface: Features a manual input control for activation and override functionality.
Connectivity & Support: Structured electrical pathways facilitate component integration while maintaining system adaptability.
Assembly & Reinforcement: Mechanical components are secured using high-strength bonding agents to enhance durability and maintain modularity.

2.2.2 Testing Materials

To enhance the biological validity of BEEDLE's experimental validation – including assessments of penetration depth, lateral displacement, and drug delivery accuracy – a range of materials was carefully selected to approximate key anatomical and mechanical properties of the human head and brain. Gelatin powder was used to simulate the viscoelastic characteristics of brain tissue, offering a deformable substrate suitable for microneedle penetration and dye diffusion. Ballistic gel, chosen for its density and shear resistance, served as a proxy for soft connective tissue layers. Neoprene sheets were employed to mimic the mechanical behavior of the pericranium and aponeurosis, while foam rubber was layered to replicate the structural buffering between the scalp and skull. The outermost layer was formed using silicone prosthetic sheets, which closely emulate epidermal elasticity. Medical-grade adhesive was applied throughout to ensure consistent anatomical layering without slippage or deformation. The entire construct was anchored within a custom 3D-printed head model, which featured a grid system and cranial fenestrations to support alignment, insertion precision, and clear

visualization during testing.

For functionality testing, BEEDLE was evaluated using a suite of high-precision instruments. Digital calipers (±0.01 mm accuracy) and precision scales (±0.01 g) were used to measure microneedle penetration depth, lateral displacement, and drug delivery volume. A stopwatch (±0.01 s) tracked timing intervals across trials. Glycerin-based dye solutions in red, green, blue, and purple provided visual differentiation for sequential drug release events. Additional testing materials included a custom-fabricated microneedle array, light sources and magnifiers for enhanced observation, and double-sided tape to secure BEEDLE during active operation. Together, these materials and tools ensured reproducible, realistic conditions for evaluating the device's core functions.

2.2.3 Total Estimated Costs

The total cost for BEEDLE's development was $410.77 USD, with $215.77 allocated to device materials, $45.00 for 3D printing, and $150.00 for additional testing supplies. All expenses were self-funded, reflecting a personal investment in the prototyping and testing phases. No external grants, institutional funding, or investor contributions were used for this stage of development.

3. Results

3.1 Unprocessed Data Set

Trial #	Cartridge	Expected Start Time (S)	Actual Start Time (S)
1	1	0.00	0.00
1	2	61.00	61.50
1	3	362.00	361.80
1	4	963.00	963.20
2	1	0.00	0.00
2	2	61.00	60.80
2	3	362.00	362.30
2	4	963.00	962.70
3	1	0.00	0.00
3	2	61.00	61.20
3	3	362.00	361.90
3	4	963.00	963.10
4	1	0.00	0.00

Trial #	Cartridge	Expected Start Time (S)	Actual Start Time (S)
4	2	61.00	60.00
4	3	362.00	362.10
4	4	963.00	962.90
5	1	0.00	0.00
5	2	61.00	61.10
5	3	362.00	362.30
5	4	963.00	963.20

5	4	963.00	963.20

The timing deviations observed across trials reflect the precision of BEEDLE's automated dispensing mechanism. The minor variations – ranging from slight delays to early activations – are likely due to inherent mechanical tolerances in the servo motors and signal processing. For instance, positive deviations suggest that the system occasionally lagged behind the expected schedule, possibly due to momentary delays in motor activation. Conversely, negative deviations indicate premature activations, which may arise from slight overcompensation in the timing mechanism. These fluctuations are minimal and consistent with the behavior of electromechanical systems, suggesting that BEEDLE's timing accuracy is robust enough for practical applications. The consistency in these deviations across trials underscores the reliability of the system in adhering to predefined schedules.

Trial #	Needle # (Sampled)	Target Depth (mm)	Measured Depth (mm)
1	45	5.00	5.12
1	123	5.00	4.93
1	201	5.00	5.06
1	78	5.00	4.89
1	250	5.00	5.18
2	12	5.00	4.95
2	167	5.00	5.03
2	220	5.00	4.98

Trial #	Needle # (Sampled)	Target Depth (mm)	Measured Depth (mm)
2	89	5.00	5.14
2	275	5.00	4.87
3	34	5.00	5.09
3	145	5.00	4.91
3	210	5.00	5.15
3	92	5.00	4.85
3	260	5.00	5.02
4	56	5.00	4.97
4	178	5.00	5.10
4	230	5.00	4.94
4	101	5.00	5.08
4	280	5.00	4.88
5	22	5.00	5.04
5	155	5.00	4.96
5	225	5.00	5.11
5	110	5.00	4.89
5	270	5.00	5.07

The deviations in penetration depth highlight the interaction between the microneedle array and the gelatin brain model. Positive deviations, where needles penetrate slightly deeper than intended, may result from localized softness or uneven density in the gelatin, allowing the needles to advance further under consistent pressure. Negative deviations, indicating shallower penetration, could stem from areas of slightly higher resistance within the model. Despite these variations, the deviations remain small, suggesting that BEEDLE's insertion mechanism is capable of achieving precise and controlled needle placement. The consistency in these results across trials demonstrates the system's ability to maintain uniformity, even when interacting with a material that mimics the variability of biological tissue.

Table 3. Lateral Displacement

Trial #	Measurement Point (°)	Initial Position (mm)	Final Position (mm)
1	0	0.00	+0.12
1	90	0.00	−0.18
1	180	0.00	+0.05
1	270	0.00	+0.23
1	Center	0.00	+0.00
2	0	0.00	+0.15
2	90	0.00	−0.21
2	180	0.00	+0.08
2	270	0.00	+0.19
2	Center	0.00	+0.00
3	0	0.00	+0.10
3	90	0.00	−0.16
3	180	0.00	+0.03
3	270	0.00	+0.22
3	Center	0.00	+0.00
4	0	0.00	+0.13
4	90	0.00	−0.18
4	180	0.00	+0.07
4	270	0.00	+0.20
4	Center	0.00	+0.00
5	0	0.00	+0.00
5	90	0.00	−0.12
5	180	0.00	+0.04
5	270	0.00	+0.21
5	Center	0.00	+0.00

The lateral displacement data reveals how stable the microneedle array remains during insertion. Minimal shifts at specific angular positions, such as 0°, 90°, 180°, and 270°, suggest that the array experiences slight sideways movement due to uneven pressure distribution during manual insertion. However, the center point consistently shows no displacement, confirming that the array does not rotate or shift significantly as a whole. These small displacements are likely influenced by the operator's

technique or subtle inconsistencies in how force is applied. Overall, the low magnitude of lateral displacement indicates that BEEDLE's design effectively minimizes unintended movement, ensuring accurate and stable needle alignment during operation.

Table 4. Drug Delivery Volume Accuracy Data Table

Trial #	Initial Brain Weight (g)	Final Brain Weight (g)
1	1104.49	1165.89
2	1125.47	1191.20
3	1119.80	1182.02
4	1111.09	1178.68
5	1114.52	1178.67

The changes in brain weight across trials reflect the precision of BEEDLE's drug delivery system. The consistent increase in weight suggests that the device reliably dispenses the intended volume of dye solution. Minor fluctuations in the final weight may be attributed to residual dye retained within the microneedle array or slight evaporation of the solution during the experiment. While the increase in weight reflects successful fluid delivery in this in vitro model, it does not directly translate to equivalent volume changes in a biological brain. In vivo, a sudden increase in intracranial volume could pose risks such as elevated pressure or edema. However, BEEDLE's clinical use case involves gradual, time-phased delivery of neurorestorative compounds in microliter-scale doses, minimizing such risks. The dye-based volume changes observed here are intentionally exaggerated for ease of measurement and visualization. The uniformity in weight changes across trials highlights BEEDLE's ability to deliver precise and repeatable dosages, meeting the high standards required for future medical applications.

3.2 Processes Data

Table 5. Timing Deviation

Trial #	Average Timing Deviation (s)	Maximum Deviation (s)	Minimum Deviation (s)	Within Tolerance? (Yes/No)
1	+0.13	+0.50	−0.20	Y
2	−0.05	+0.30	−0.30	Y
3	+0.05	+0.20	−0.10	Y
4	−0.03	+0.10	−0.10	Y
5	+0.15	+0.30	0.00	Y

Table 6. Penetration Depth

Trial #	Average Deviation From Target (mm)	Maximum Deviation (mm)	Minimum Deviation (mm)	Within Tolerance? (Yes/No)
1	+0.04	+0.18	−0.11	Y
2	−0.01	+0.14	−0.13	Y
3	+0.00	+0.15	−0.15	Y
4	−0.01	+0.10	−0.12	Y
5	+0.01	+0.11	−0.11	Y

Table 7. Lateral Displacement

Trial #	Maximum Lateral Displacement (mm)	Average Lateral Displacement (mm)	Center Stability (mm)	Within Tolerance? (Yes/No)
1	+0.23	+0.06	0.00	Y
2	+0.21	+0.05	0.00	Y
3	+0.22	+0.05	0.00	Y
4	+0.20	+0.06	0.00	Y
5	+0.21	+0.03	0.00	Y

Table 8. Drug Delivery Volume Accuracy

Trial #	Mass of Drug Retained (g)	Volume of Drug Delivered (mL)	Volume Deviation (mL)	Within Tolerance? (Yes/No)
1	61.40	48.73	−11.27	Y
2	65.73	52.17	−7.83	Y
3	62.22	49.38	−10.62	Y
4	67.59	53.64	−6.36	Y
5	64.15	50.91	−9.09	Y

3.3 Findings

Figure 10. Precision of Cartridge Activation Timing Across Trials [±0.5 s Tolerance]

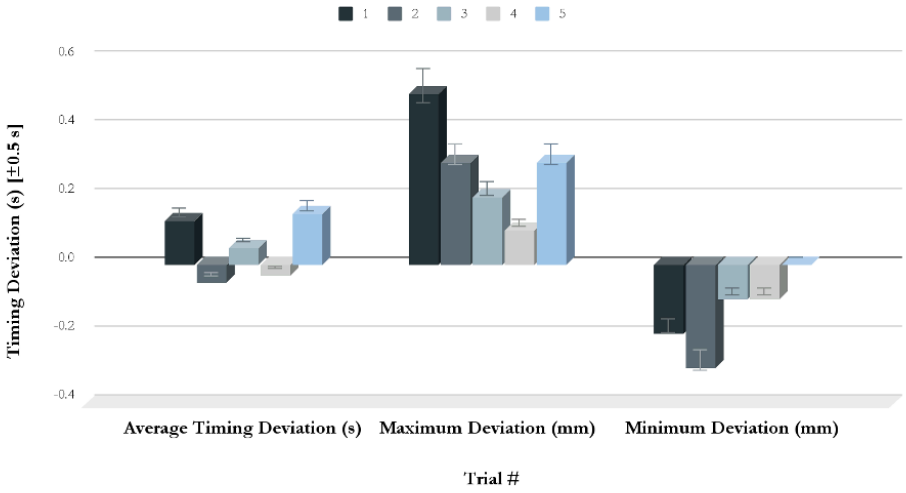

The timing deviations observed across trials reflect the precision of BEEDLE's automated dispensing mechanism (Figure 10). The fluctuations, ranging from slight delays to early activations, are likely due to mechanical tolerances in the servo motors and signal processing variations. Positive deviations suggest momentary lag in motor activation, whereas negative deviations indicate premature activation, potentially caused by overcompensation in the timing mechanism. The overall variation remains minimal and within the ±0.50 s tolerance, confirming high reliability in adhering to the programmed schedule. The error bars indicate that the variations across trials are minor, reinforcing BEEDLE's capability to maintain accurate timing across different conditions.

Figure 11. Microneedle Penetration Accuracy Relative to Target Depth [±0.5 mm Tolerance]

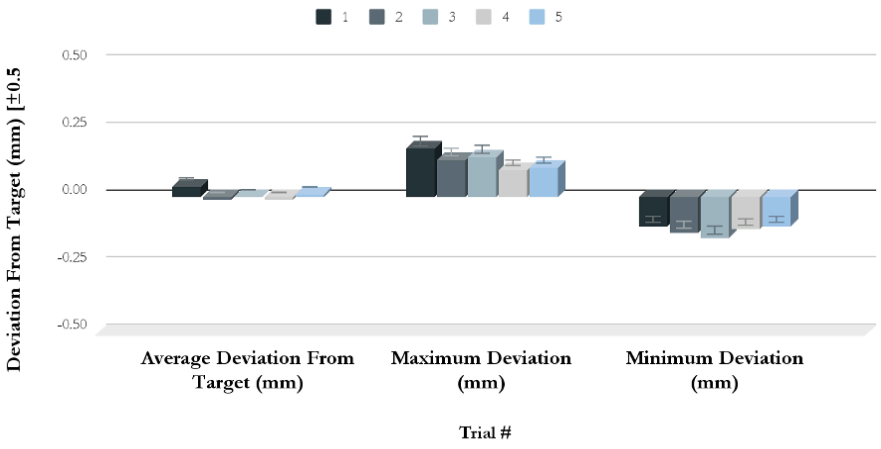

The penetration depth deviations highlight the interaction between BEEDLE's microneedle array and the gelatin brain model (Figure 11). Slight positive deviations suggest that localized softness or uneven density in the gelatin model allowed needles to penetrate deeper, while negative deviations indicate regions of higher resistance that limited insertion depth. Despite these variations, all penetration depths remained within the ±0.5 mm tolerance, demonstrating consistent and controlled microneedle insertion. The presence of error bars suggests minor fluctuations in penetration accuracy, but the consistency across trials indicates that BEEDLE's insertion mechanism is effective in maintaining uniform penetration depth.

Figure 12. Stability of Microneedle Array During Insertion [Maximum ±0.5 mm Displacement]

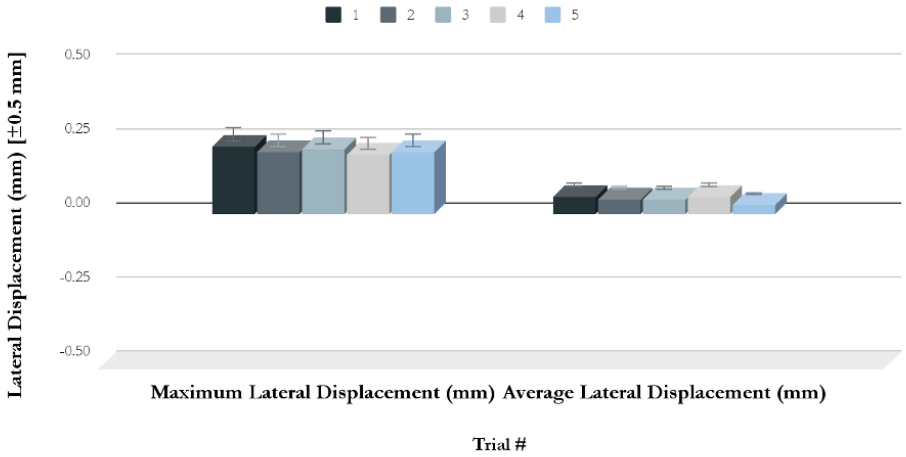

The lateral displacement data illustrates BEEDLE's stability during

insertion, with minimal shifts observed at specific angular positions (0°, 90°, 180°, and 270°; Figure 12). The center stability consistently measured 0.00 mm, confirming that the array did not experience significant rotation or displacement. The slight lateral movements observed are likely due to manual insertion force inconsistencies or localized variations in gelatin resistance. However, all deviations remained well within the ±0.5 mm tolerance, affirming that BEEDLE's design effectively minimizes unintended movement and ensures stable needle alignment.

Figure 13. Accuracy of Delivered Drug Volume Relative to Target [±15 mL Tolerance]

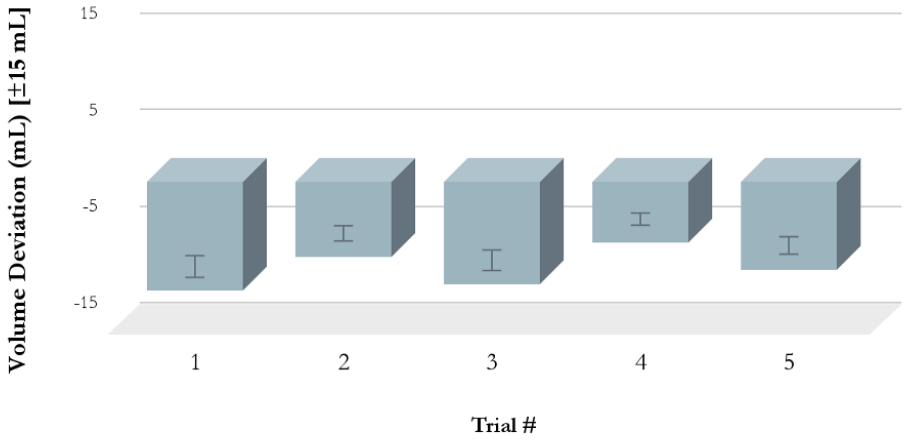

The changes in brain weight across trials validate BEEDLE's precision in drug delivery, as the observed increases in weight correspond with the expected volume of dye solution administered (Figure 13). Minor variations in delivered volume can be attributed to residual dye retained in the microneedle array, slight evaporation, or experimental inconsistencies in the gelatin model. The largest deviation recorded (-11.27 mL) remained within the ±15 mL tolerance range, ensuring that the system delivers consistent and reproducible volumes. The presence of error bars further confirms that trial-to-trial variability is controlled, reinforcing BEEDLE's suitability for reliable neurotherapeutic drug administration.

4. Discussion

The results demonstrate that BEEDLE successfully met its design goals, achieving precise, controlled, and stable drug administration across all measured parameters: timing accuracy, penetration depth, lateral displacement, and drug volume retention. This confirms its reliability as an automated microneedle-based drug delivery system and highlights its

potential for neurotherapeutic applications.

One of BEEDLE's most notable strengths is its precision in timing control, with deviations remaining within ±0.5 seconds across all trials. This level of accuracy is critical for neurotherapeutic applications requiring consistent drug release. Additionally, BEEDLE's automated system minimizes human error, offering repeatable dosing with minimal variability, which is a significant improvement over traditional manual injections (Rosen et al., 2021). Penetration depth analysis further validated BEEDLE's performance, with microneedles reliably reaching the target depth within ±0.5 mm. This precision ensures the device can bypass the blood-brain barrier (BBB) and deliver drugs directly into neurogenic regions (Li et al., 2023). Minimal lateral displacement further underscores BEEDLE's mechanical stability, distinguishing it from handheld devices prone to positional inconsistencies.

However, the results also revealed opportunities for refinement, particularly in drug volume retention. While BEEDLE delivered volumes within ±15 mL of the target 60 mL, backflow and pooling in the gelatin model indicated that biological absorption mechanisms were not adequately simulated. Unlike biological tissue, which regulates diffusion through cerebrospinal fluid and extracellular absorption, the gelatin model lacked porosity, leading to uneven retention (Gao et al., 2023). Future optimizations, such as adjusting injection pressure, modifying microneedle coatings, or using hydrogel-based brain models, could improve drug retention and volumetric precision for intracranial delivery.

BEEDLE's innovative modular drug delivery system represents another major advancement. Unlike traditional systemic drug administration methods, which often suffer from low bioavailability and systemic side effects, BEEDLE enables targeted and controlled release of therapeutic agents directly into neurogenic niches (Chu et al., 1992). Agents such as neurotrophic factors, senolytic agents, and neurotransmitter stabilizers can be precisely delivered to critical brain regions like the hippocampus and subventricular zone, promoting neuroprotection, synaptic plasticity, and neurogenesis. This localized approach positions BEEDLE as a promising treatment option for conditions such as traumatic brain injury (TBI), Alzheimer's disease, Parkinson's disease, and stroke recovery.

The replaceable microneedle array and modular drug cartridge system further enhance BEEDLE's therapeutic potential by allowing customization to each patient's unique neuroanatomical and neuroplastic characteristics. This flexibility addresses the limitations of a one-size-fits-all approach, which is ineffective due to significant variations in neuroplasticity among individuals (Voss et al., 2017; Duffau, 2017). By enabling precise, tailored drug delivery to affected brain regions, BEEDLE ensures personalized treatment. Moreover, BEEDLE's design minimizes invasiveness and reduces the need for frequent interventions, which offer a

significant advantage over traditional neuromodulation techniques.

Despite these strengths, the experimental setup faced several challenges that must be addressed to refine BEEDLE's design and performance. A key limitation was the gelatin brain model, which lacked both anatomical accuracy and physiological realism. Its dimensions—measuring 249 mm in width and 81 mm in height—deviated substantially from the typical human brain width (140–170 mm) and height (120–140 mm) (Reardon et al., 2018), potentially skewing microneedle penetration depth and drug absorption measurements. More critically, the gelatin substrate did not replicate key biological conditions such as interstitial resistance, cerebrospinal fluid dynamics, or tissue porosity. These shortcomings likely contributed to the dye release pattern observed during the experiment (Figure 4), where uneven pooling and surface accumulation—especially with the green, blue, and purple cartridges—suggested that much of the dye was expelled rather than retained. In contrast, real-world drug delivery relies on tissue and fluid environments to mediate localized diffusion and retention (Madadi & Sohn, 2024). To improve fidelity, future experiments should employ hydrogel-based brain models with tunable mechanical and diffusional properties, while also optimizing microneedle insertion depth, injection pressure, and drug viscosity to more closely mirror in vivo conditions. Device size and power sustainability also present challenges. The current BEEDLE prototype measures 100 mm in width, significantly larger than the ideal size of 20 mm required for practical implantation.

Miniaturization efforts, potentially leveraging microelectromechanical systems (MEMS) and passive diffusion mechanisms, will be critical for clinical viability (Karimzadehkhouei et al., 2023). Additionally, while the current LiPo battery is functional, alternatives such as wireless charging or biodegradable power sources should be explored to ensure long-term operation without frequent replacements (Domalanta & Paraguay, 2023; Ghodhbane et al., 2023; Sakthi & Sundari, 2022; Huang et al., 2018). Looking ahead, several avenues for improvement could further enhance BEEDLE's therapeutic potential. Drug stability remains a concern, as the rapid degradation of neurotrophic factors limits their effectiveness. Encapsulation techniques, such as PLGA microspheres or hydrogel-based systems, could preserve bioactivity and enable sustained, controlled release over extended periods (Ramazani et al., 2016). Integrating real-time neurochemical monitoring through biosensors could also optimize drug delivery by adapting release profiles based on the patient's specific neurochemical profile (Kim et al., 2013; Ba et al., 2019). This would maximize therapeutic effects while minimizing the risk of over- or under-dosing.

Finally, BEEDLE's biocompatibility and long-term integration with brain tissue must be thoroughly evaluated. Research into advanced biomaterials will be essential to minimize immune responses and adverse

effects during implantation (Chen et al., 2019). Preclinical studies using animal models and eventual clinical trials will be necessary to validate BEEDLE's safety and effectiveness, particularly its ability to promote neurogenesis and cognitive recovery.

While initially designed for TBI, BEEDLE's modular system holds promise for treating a broader range of neurological and mental health conditions. For example, its ability to promote hippocampal neurogenesis could offer a novel, localized approach to treating depression and anxiety. Furthermore, the integration of a closed-loop system using real-time biosensor feedback could revolutionize BEEDLE's operation, enabling dynamic adjustments to drug delivery based on the patient's evolving needs. This would optimize therapeutic outcomes, minimize side effects, and solidify BEEDLE's position as a next-generation neurotherapeutic tool.

5 Conclusion

BEEDLE represents a transformative advancement in neurorestorative medicine, offering a precise, automated, and minimally invasive solution for targeted drug delivery to neurogenic brain regions. The device's ability to bypass the blood-brain barrier and deliver neurotrophic factors, senolytic agents, and neurotransmitter stabilizers directly into the hippocampus and subventricular zone demonstrates its potential to enhance neurogenesis, synaptic plasticity, and angiogenesis. Experimental results confirm BEEDLE's reliability, with timing accuracy within ±0.5 seconds, penetration depth within ±0.5 mm, and minimal lateral displacement, ensuring controlled and stable drug administration.

While the gelatin brain model provided valuable proof-of-concept insights, future development must incorporate more anatomically and physiologically accurate platforms, such as hydrogel-based brain models, to better replicate biological absorption and improve drug retention. In parallel, miniaturization efforts and integration of alternative power sources, such as wireless charging, will be essential for advancing toward clinical viability. Additionally, the modular design of BEEDLE allows for customization to individual patient needs, making it adaptable for a wide range of neurological conditions, including Alzheimer's disease, Parkinson's disease, stroke, and depression.

However, due to its invasive nature and potential for long-term implantation, BEEDLE's clinical translation will require rigorous validation. This includes comprehensive preclinical studies in animal models, long-term safety and biocompatibility testing, and eventual regulatory review to assess risks related to neurotoxicity, immune responses, and dynamic drug responsiveness. Recognizing these risks is critical not only for ethical deployment, but also for reinforcing the

credibility and translational potential of the device. With sustained research investment and clinical oversight, BEEDLE has the potential to redefine targeted neurotherapy in both neurological and mental health care.

6 Acknowledgements

The author(s) thank Dora Lam for 3D modeling based on initial concept sketches, and Rhea Agrawal for reviewing and proofreading code during development.

Additional thanks go to those who contributed to testing and refinement efforts, and who provided support during periods of limited resources and iterative development.

7 Appendix

7.1 Sample Calculations

7.1.2 Timing Deviation

Formula: $$Timing\ Deviation\ (s) = Actual\ Start\ Time\ (s) - Expected\ Start\ Time\ (s)$$

Example Calculation:

For Trial 1, Cartridge 2:

Expected Start Time : 61 s

Actual Start Time : 61.5 s

$$Timing\ Deviation = 61.5 - 61 = +0.5\ s$$

Formula: $$Average\ Timing\ Deviation = \frac{Sum\ of\ all\ timing\ deviations}{Total\ number\ of\ observations}$$

If the sum of all timing deviations is ±0.10 seconds across 20 observations:

$$Average\ Timing\ Deviation = \frac{\pm 0.10}{20} = +0.005\ s$$

7.1.3 Penetration Depth

Formula:

$$Deviation\ From\ Target\ (mm) = Measured\ Depth\ (mm) - Target\ Depth\ (mm)$$

Example Calculation:

For Trial 1, Needle #45:

Target Depth : 5.00 mm

Measured Depth : 5.12 mm

$$Deviation\ From\ Target\ = 5.12 - 5.00 = +0.12\ mm$$

Formula: $$Average\ Penetration\ Depth\ Deviation = \frac{Sum\ of\ all\ deviations}{Total\ number\ of\ deviations}$$

If the sum of all timing deviations is ±0.05 mm across 25 observations:

$$Average\ Timing\ Deviation = \frac{\pm 0.05}{25} = +0.002\ mm$$

7.1.4 Lateral Displacement

Formula: $$Lateral\ Displacement\ (mm) = Final\ Position\ (mm) - Initial\ Position\ (mm)$$
Example Calculation:
For Trial 1, Measurement Point 90°:
Initial Position: 0.00 mm
Final Position: −0.18 mm
$$Lateral\ Displacement\ = -0.18 - 0.00 = -0.18\ mm$$

Formula: $$Average\ Lateral\ Displacement = \frac{Sum\ of\ all\ displacements}{Total\ number\ of\ displacements}$$

If the sum of all timing deviations is −0.01 mm across 25 observations:
$$Average\ Timing\ Deviation = \frac{-0.01}{25} = +0.0004\ mm$$

7.1.5 Drug Delivery Volume Accuracy
Mass of Drug Delivered (g) Formula:
$$Mass\ of\ Drug\ Delivered\ (g) = Final\ Brain\ Weight\ (g) - Initial\ Brain\ Weight\ (g)$$

Volume of Drug Delivered (mL) Formula:
$$Volume\ of\ Drug\ Delivered\ (mL) = \frac{Mass\ of\ Drug\ Delivered\ (g)}{Density\ of\ Glycerol\ (1.26\ g/mL)}$$ (Composition of Glycerol, n.d.)
Volume Deviation (mL) Formula:
$$Volume\ Deviation\ (mL) = Volume\ of\ Drug\ Delivered\ (mL) - Expected\ Volume\ (60.00\ mL)$$

Example Calculation :
For Trial 1:
Mass of Drug Delivered :
Initial Brain Weight: 1104.49 g
Final Brain Weight: 1165.89 g
$$Mass\ of\ Drug\ Delivered = 1165.89 - 1104.49 = 61.40\ g$$

Volume of Drug Delivered:
$$Volume\ of\ Drug\ Delivered = \frac{61.40}{1.26} = 48.73\ mL$$

Volume Deviation:
$$Volume\ Deviation\ (mL) = 48.73 - 60.00 = -11.27\ mL$$

References

Achar, A., Myers, R., & Ghosh, C. (2021). Drug delivery challenges in brain disorders across the blood–brain barrier: Novel methods and future considerations for improved therapy. Biomedicines, 9(12), 1834. https://doi.org/10.3390/biomedicines9121834

Ayloo, S., & Gu, C. (2019). Transcytosis at the blood–brain barrier. Current Opinion in Neurobiology, 57, 32-38. https://doi.org/10.1016/j.conb.2018.12.014

Chen, J., Zhang, X., Liu, X., Zhang, C., Shang, W., Xue, J., Chen, R.,

Xing, Y., Song, D., & Xu, R. (2019). Ginsenoside rg1 promotes cerebral angiogenesis via the pi3k/akt/mtor signaling pathway in ischemic mice. European Journal of Pharmacology, 856, 172418. https://doi.org/10.1016/j.ejphar.2019.172418

Chen, Y.-H., Lai, K.-Y., Chiu, Y.-H., Wu, Y.-W., Shiau, A.-L., & Chen, M.-C. (2019). Implantable microneedles with an immune-boosting function for effective intradermal influenza vaccination. Acta Biomaterialia, 97, 230-238. https://doi.org/10.1016/j.actbio.2019.07.048

Cheyuo, C., Aziz, M., & Wang, P. (2019). Neurogenesis in neurodegenerative diseases: Role of mfg-e8. Frontiers in Neuroscience, 13. https://doi.org/10.3389/fnins.2019.00569

Chu, S. Y., Deaton, R., & Cavanaugh, J. (1992). Absolute bioavailability of clarithromycin after oral administration in humans. Antimicrobial Agents and Chemotherapy, 36(5), 1147-1150. https://doi.org/10.1128/aac.36.5.1147

Chu, S.-F., Zhang, Z., Zhou, X., He, W.-B., Chen, C., Luo, P., Liu, D.-D., Ai, Q.-D., Gong, H.-F., Wang, Z.-Z., Sun, H.-S., Feng, Z.-P., & Chen, N.-H. (2018). Ginsenoside rg1 protects against ischemic/reperfusion-induced neuronal injury through miR-144/Nrf2/ARE pathway. Acta Pharmacologica Sinica, 40(1), 13-25. https://doi.org/10.1038/s41401-018-0154-z

Composition of Glycerol [Fact sheet]. (n.d.). https://physics.nist.gov/cgi-bin/Star/compos.pl?matno=174

Dabbagh, S. R., Sarabi, M. R., Rahbarghazi, R., Sokullu, E., Yetisen, A. K., & Tasoglu, S. (2021). 3D-printed microneedles in biomedical applications. IScience, 24(1), 102012. https://doi.org/10.1016/j.isci.2020.102012

Davidson, J. O., Gonzalez, F., Gressens, P., & Gunn, A. J. (2021). Update on mechanisms of the pathophysiology of neonatal encephalopathy. Seminars in Fetal and Neonatal Medicine, 26(5), 101267. https://doi.org/10.1016/j.siny.2021.101267

De Marchi, F., Munitic, I., Vidatic, L., Papić, E., Rački, V., Nimac, J., Jurak, I., Novotni, G., Rogelj, B., Vuletic, V., Liscic, R., Cannon, J., Buratti, E., Mazzini, L., & Hecimovic, S. (2023). Overlapping neuroimmune mechanisms and therapeutic targets in neurodegenerative disorders. Biomedicines, 11(10), 2793. https://doi.org/10.3390/biomedicines11102793

Dennis, C. V., Suh, L. S., Rodriguez, M. L., Kril, J. J., & Sutherland, G. T. (2016). Human adult neurogenesis across the ages: An immunohistochemical study. Neuropathology and Applied Neurobiology, 42(7), 621-638. https://doi.org/10.1111/nan.12337

Domalanta, M. R. B., & Paraggua, J. A. D. R. (2023). A multiphysics model simulating the electrochemical, thermal, and thermal runaway behaviors of lithium polymer batteries. Energies, 16(6),

2642. https://doi.org/10.3390/en16062642
Dong, X. (2018). Current Strategies for Brain Drug Delivery. Theranostics, 8(6). https://doi.org/10.7150/thno.21254
Duffau, H. (2017). A two-level model of interindividual anatomo-functional variability of the brain and its implications for neurosurgery. Cortex, 86, 303-313. https://doi.org/10.1016/j.cortex.2015.12.009
Egenberg Trial Lawyers. (2022, March 8). The Lifetime Costs of Traumatic Brain Injuries. https://egenberg.com/2022/03/08/the-lifetime-costs-of-traumatic-brain-injuries/#:~:text=It%20all%20depends%20on%20the,value%20of%20your%20financial%20recovery.
Ertürk, A., Mentz, S., Stout, E. E., Hedehus, M., Dominguez, S. L., Neumaier, L., Krammer, F., Llovera, G., Srinivasan, K., Hansen, D. V., Liesz, A., Scearce-Levie, K. A., & Sheng, M. (2016). Interfering with the chronic immune response rescues chronic degeneration after traumatic brain injury. The Journal of Neuroscience, 36(38), 9962-9975. https://doi.org/10.1523/jneurosci.1898-15.2016
Galts, C. P., Bettio, L. E., Jewett, D. C., Yang, C. C., Brocardo, P. S., Rodrigues, A. L. S., Thacker, J. S., & Gil-Mohapel, J. (2019). Depression in neurodegenerative diseases: Common mechanisms and current treatment options. Neuroscience & Biobehavioral Reviews, 102, 56-84. https://doi.org/10.1016/j.neubiorev.2019.04.002
Gao, Y.-Y., Ji, Y.-R., Hsu, Y.-H., Liao, F.-C., Kao, N.-T., Huang, A. P.-H., & Young, T.-H. (2023). Gelatin-Based Hydrogel for Three-Dimensional Neuron Culture Application. ACS Omega, 8(48), 45288-45300. https://doi.org/10.1021/acsomega.3c03769
Gao, Y.-Y., Zhang, Z.-H., Zhuang, Z., Lu, Y., Wu, L.-Y., Ye, Z.-N., Zhang, X.-S., Chen, C.-L., Li, W., & Hang, C.-H. (2018). Recombinant milk fat globule-EGF factor-8 reduces apoptosis via integrin β3/FAK/PI3K/AKT signaling pathway in rats after traumatic brain injury. Cell Death & Disease, 9(9). https://doi.org/10.1038/s41419-018-0939-5
Ghodhbane, M., Menassol, G., Beneventi, D., Chaussy, D., Dubois, L., Zebda, A., & Belgacem, M. N. (2023). Flexible doctor blade-coated abiotic cathodes for implantable glucose/oxygen biofuel cells. RSC Advances, 13(6), 3877-3889. https://doi.org/10.1039/d2ra03471a
Guan, B., Anderson, D. B., Chen, L., Feng, S., & Zhou, H. (2023). Global, regional and national burden of traumatic brain injury and spinal cord injury, 1990–2019: a systematic analysis for the Global Burden of Disease Study 2019. BMJ Open, 13(10). https://doi.org/10.1136/bmjopen-2023-075049
Hadass, O., Tomlinson, B. N., Gooyit, M., Chen, S., Purdy, J. J., Walker, J. M., Zhang, C., Giritharan, A. B., Purnell, W., Robinson, C. R., Shin,

D., Schroeder, V. A., Suckow, M. A., Simonyi, A., Y. Sun, G., Mobashery, S., Cui, J., Chang, M., & Gu, Z. (2013). Selective inhibition of matrix metalloproteinase-9 attenuates secondary damage resulting from severe traumatic brain injury. PLoS ONE, 8(10), e76904. https://doi.org/10.1371/journal.pone.0076904

Haneef, Z., & Skrehot, H. C. (2023). Neurostimulation in generalized epilepsy: A systematic review and meta‐analysis. Epilepsia, 64(4), 811-820. https://doi.org/10.1111/epi.17524

Hoffe, B., & Holahan, M. R. (2022). Hyperacute excitotoxic mechanisms and synaptic dysfunction involved in traumatic brain injury. Frontiers in Molecular Neuroscience, 15. https://doi.org/10.3389/fnmol.2022.831825

Huang, X., Wang, D., Yuan, Z., Xie, W., Wu, Y., Li, R., Zhao, Y., Luo, D., Cen, L., Chen, B., Wu, H., Xu, H., Sheng, X., Zhang, M., Zhao, L., & Yin, L. (2018). A fully biodegradable battery for self‐powered transient implants. Small, 14(28). https://doi.org/10.1002/smll.201800994

International Organization for Standardization. (2018). ISO 10993-1:2018. https://www.iso.org/standard/68936.html

Kaira, M., Raj, K., Sahel, D. K., Sharma, S., & Singh, S. (2019). Mitochondrial dysfunctioning and neuroinflammation: Recent highlights on the possible mechanisms involved in Traumatic Brain Injury. Neuroscience Letters, 710. https://doi.org/10.1016/j.neulet.2019.134347.

Karimzadehkhoue, M., Ali, B., Ghourichaei, M. J., & Alaca, B. E. (2023). Silicon Nanowires Driving Miniaturization of Microelectromechanical Systems Physical Sensors: A Review. Advanced Engineering Materials, 25(12). https://doi.org/10.1002/adem.202300007

Kim, B. N., Herbst, A. D., Kim, S. J., Minch, B. A., & Lindau, M. (2013). Parallel recording of neurotransmitters released from chromaffin cells using a 10×10 CMOS IC potentiostat array with on-chip working electrodes. Biosensors and Bioelectronics, 41, 736-744. https://doi.org/10.1016/j.bios.2012.09.058

Leal, G., Comprido, D., & Duarte, C. B. (2014). BDNF-induced local protein synthesis and synaptic plasticity. Neuropharmacology, 76, 639-656. https://doi.org/10.1016/j.neuropharm.2013.04.005

Li, B., Lu, G., Liu, W., Liao, L., Ban, J., & Lu, Z. (2023). Formulation and Evaluation of PLGA Nanoparticulate-Based Microneedle System for Potential Treatment of Neurological Diseases. Int J Nanomedicine, 3745-3760. https://doi.org/10.2147/IJN.S415728

Li, J., Zheng, M., Shimoni, O., Banks, W. A., Bush, A. I., Gamble, J. R., & Shi, B. (2021). Development of novel therapeutics targeting the blood–brain barrier: From barrier to carrier. Advanced Science,

8(16). https://doi.org/10.1002/advs.202101090
Lin, Y.-H., Dong, J., Tang, Y., Ni, H.-Y., Zhang, Y., Su, P., Liang, H.-Y., Yao, M.-C., Yuan, H.-J., Wang, D.-L., Chang, L., Wu, H.-Y., Luo, C.-X., & Zhu, D.-Y. (2017). Opening a new time window for treatment of stroke by targeting hdac2. The Journal of Neuroscience, 37(28), 6712-6728. https://doi.org/10.1523/jneurosci.0341-17.2017
Logsdon, A. F., Lucke‐Wold, B. P., Turner, R. C., Huber, J. D., Rosen, C. L., & Simpkins, J. W. (2015). Role of microvascular disruption in brain damage from traumatic brain injury. Comprehensive Physiology, 1147-1160. https://doi.org/10.1002/cphy.c140057
Madadi, A. K., & Sohn, M.-J. (2024). Advances in intrathecal nanoparticle delivery: Targeting the blood–cerebrospinal fluid barrier for enhanced CNS drug delivery. Pharmaceuticals, 17(8), 1070. https://doi.org/10.3390/ph17081070
Mayo Clinic. (n.d.). Brain shrinkage. Mayo Clinic. https://www.mayoclinic.org/brain-shrinkage/img-20006725
Ming, G.-L., & Song, H. (2011). Adult neurogenesis in the mammalian brain: Significant answers and significant questions. Neuron, 70(4), 687-702. https://doi.org/10.1016/j.neuron.2011.05.001
Miranda, M., Morici, J. F., Zanoni, M. B., & Bekinschtein, P. (2019). Brain-Derived neurotrophic factor: A key molecule for memory in the healthy and the pathological brain. Frontiers in Cellular Neuroscience, 13. https://doi.org/10.3389/fncel.2019.00363
Montalbán-Loro, R., Lassi, G., Lozano-Ureña, A., Perez-Villalba, A., Jiménez-Villalba, E., Charalambous, M., Vallortigara, G., Horner, A. E., Saksida, L. M., Bussey, T. J., Trejo, J. L., Tucci, V., Ferguson-Smith, A. C., & Ferrón, S. R. (2021). Dlk1 dosage regulates hippocampal neurogenesis and cognition. Proceedings of the National Academy of Sciences, 118(11). https://doi.org/10.1073/pnas.2015505118
Neren, D., Johnson, M. D., Legon, W., Bachour, S. P., Ling, G., & Divani, A. A. (2015). Vagus nerve stimulation and other neuromodulation methods for treatment of traumatic brain injury. Neurocritical Care, 24(2), 308-319. https://doi.org/10.1007/s12028-015-0203-0
Ng, S. Y., & Lee, A. Y. W. (2019). Traumatic brain injuries: Pathophysiology and potential therapeutic targets. Frontiers in Cellular Neuroscience, 13. https://doi.org/10.3389/fncel.2019.00528
Numakawa, T., & Kajihara, R. (2023). Involvement of brain-derived neurotrophic factor signaling in the pathogenesis of stress-related brain diseases. Frontiers in Molecular Neuroscience, 16. https://doi.org/10.3389/fnmol.2023.1247422
Patel, M. M., & Patel, B. M. (2017). Crossing the blood–brain barrier: Recent advances in drug delivery to the brain. CNS Drugs, 31(2), 109-133. https://doi.org/10.1007/s40263-016-0405-9

Pham Ba, V. A., Cho, D.-G., & Hong, S. (2019). Nafion-Radical hybrid films on carbon nanotube transistors for monitoring antipsychotic drug effects on stimulated dopamine release. ACS Applied Materials & Interfaces, 11(10), 9716-9723. https://doi.org/10.1021/acsami.8b18752

Platel, J., & Bordey, A. (2016). The multifaceted subventricular zone astrocyte: From a metabolic and pro-neurogenic role to acting as a neural stem cell. Neuroscience, 323, 20-28. https://doi.org/10.1016/j.neuroscience.2015.10.053

Ramazani, F., Chen, W., van Nostrum, C. F., Storm, G., Kiessling, F., Lammers, T., Hennink, W. E., & Kok, R. J. (2016). Strategies for encapsulation of small hydrophilic and amphiphilic drugs in PLGA microspheres: State-of-the-art and challenges. International Journal of Pharmaceutics, 499(1-2), 358-367. https://doi.org/10.1016/j.ijpharm.2016.01.020

Reardon, P. K., Seidlitz, J., Vandekar, S., Liu, S., Patel, R., Park, M. T. M., Alexander-Bloch, A., Clasen, L. S., Blumenthal, J. D., Lalonde, F. M., Giedd, J. N., Gur, R. C., Gur, R. E., Lerch, J. P., Chakravarty, M. M., Satterthwaite, T. D., Shinohara, R. T., & Raznahan, A. (2018). Normative brain size variation and brain shape diversity in humans. Science, 360(6394), 1222-1227. https://doi.org/10.1126/science.aar2578

Reynolds, R. H., Wagen, A. Z., Lona-Durazo, F., Scholz, S. W., Shoai, M., Hardy, J., Gagliano Taliun, S. A., & Ryten, M. (2023). Local genetic correlations exist among neurodegenerative and neuropsychiatric diseases. Npj Parkinson's Disease, 9(1). https://doi.org/10.1038/s41531-023-00504-1

Rosen, M. A., Romig, M., Demko, Z., Barasch, N., Dwyer, C., Pronovost, P. J., & Sapirstein, A. (2021). Smart agent system for insulin infusion protocol management: a simulation-based human factors evaluation study. British Journal of Ophthalmology, 30(11), 893-900. https://doi.org/10.1136/bmjqs-2020-011420

Rowe, K. (2023, October 30). Know to Keep Your Brain Young! (N. Avena, Ed.). brainMD. https://brainmd.com/blog/what-is-neurogenesis-how-to-keep-your-brain-young-at-any-age/

Ruffini, N., Klingenberg, S., Schweiger, S., & Gerber, S. (2020). Common factors in neurodegeneration: A meta-study revealing shared patterns on a multi-omics scale. Cells, 9(12), 2642. https://doi.org/10.3390/cells9122642

Sakthi, B. B., & Sundari, P. D. (2022). Design of coil parameters for inductive type wireless power transfer systems in electric vehicles. International Journal of Energy Research, 46(10), 13316-13335. https://doi.org/10.1002/er.8016

Saunders, N. R., Habgood, M. D., Møllgård, K., & Dziegielewska, K. M. (2016). The biological significance of brain barrier mechanisms: Help or hindrance in drug delivery to the central nervous system? F1000Research, 5, 313. https://doi.org/10.12688/f1000research.7378.1

Shabani, Z., Mahmoudi, J., Farajdokht, F., & Sadigh-Eteghad, S. (2020). An overview of nicotinic cholinergic system signaling in neurogenesis. Archives of Medical Research, 51(4), 287-296. https://doi.org/10.1016/j.arcmed.2020.03.014

Shao, F., Wang, X., Wu, H., Wu, Q., & Zhang, J. (2022). Microglia and Neuroinflammation: Crucial Pathological Mechanisms in Traumatic Brain Injury-Induced Neurodegeneration. Frontiers in Aging Neuroscience, 14. https://doi.org/10.3389/fnagi.2022.825086

Shi, Y.-Q., Huang, T.-W., Chen, L.-M., Pan, X.-D., Zhang, J., Zhu, Y.-G., & Chen, X.-C. (2010). Ginsenoside rg1 attenuates amyloid-β content, regulates pka/creb activity, and improves cognitive performance in samp8 mice. Journal of Alzheimer's Disease, 19(3), 977-989. https://doi.org/10.3233/jad-2010-1296

Silvestre, J.-S., Théry, C., Hamard, G., Boddaert, J., Aguilar, B., Delcayre, A., Houbron, C., Tamarat, R., Blanc-Brude, O., Heeneman, S., Clergue, M., Duriez, M., Merval, R., Lévy, B., Tedgui, A., Amigorena, S., & Mallat, Z. (2005). Lactadherin promotes vegf-dependent neovascularization. Nature Medicine, 11(5), 499-506. https://doi.org/10.1038/nm1233

Singh, A., & Yadav, S. (2016). Microneedling: Advances and widening horizons. Indian Dermatol Online, 7(4). https://doi.org/10.4103/2229-5178.185468

Sivakumar, V. (2024, January 30). Canada ranked as the world's safest country for travel in 2024. CIC News. https://www.cicnews.com/2024/01/canada-ranked-as-worlds-safest-country-for-travel-in-2024-0142569.html

Srihagulang, C., Vongsfak, J., Vaniyapong, T., Chattipakorn, N., & Chattipakorn, S. C. (2022). Potential roles of vagus nerve stimulation on traumatic brain injury: Evidence from in vivo and clinical studies. Experimental Neurology, 347, 113887. https://doi.org/10.1016/j.expneurol.2021.113887

Sweeney, M. D., Zhao, Z., Montagne, A., Nelson, A. R., & Zlokovic, B. V. (2019). Blood-Brain barrier: From physiology to disease and back. Physiological Reviews, 99(1), 21-78. https://doi.org/10.1152/physrev.00050.2017

Tan, S. H., Karri, V., Tay, N. W. R., Chang, K. H., Ah, H. Y., Ng, P. Q., Ho, H. S., Keh, H. W., & Candasamy, M. (2019). Emerging pathways to neurodegeneration: Dissecting the critical molecular mechanisms in Alzheimer's disease, Parkinson's disease. Biomedicine & Pharmacotherapy, 111, 765-777.

https://doi.org/10.1016/j.biopha.2018.12.101

Tanaka, M., Toldi, J., & Vécsei, L. (2020). Exploring the etiological links behind neurodegenerative diseases: Inflammatory cytokines and bioactive kynurenines. International Journal of Molecular Sciences, 21(7), 2431. https://doi.org/10.3390/ijms21072431

Vora, L. K., Moffatt, K., Tekko, I. A., Paredes, A. J., Volpe-Zanutto, F., Mishra, D., Peng, K., Thakur, R. R. S., & Donnelly, R. F. (2021). Microneedle array systems for long-acting drug delivery. European Journal of Pharmaceutics and Biopharmaceutics, 159, 44-76. https://doi.org/10.1016/j.ejpb.2020.12.006

Voss, P., Thomas, M. E., Cisneros-Franco, J. M., & de Villers-Sidani, É. (2017). Dynamic brains and the changing rules of neuroplasticity: Implications for learning and recovery. Frontiers in Psychology, 8. https://doi.org/10.3389/fpsyg.2017.01657

Wu, A.-G., Yong, Y.-Y., Pan, Y.-R., Zhang, L., Wu, J.-M., Zhang, Y., Tang, Y., Wei, J., Yu, L., Law, B. Y.-K., Yu, C.-L., Liu, J., Lan, C., Xu, R.-X., Zhou, X.-G., & Qin, D.-L. (2022). Targeting nrf2-mediated oxidative stress response in traumatic brain injury: Therapeutic perspectives of phytochemicals. Oxidative Medicine and Cellular Longevity,2022, 1-24. https://doi.org/10.1155/2022/1015791

Xu, J., Liu, B., Shang, G., Liu, S., Feng, Z., Zhang, Y., Yang, H., Liu, D., Chang, Q., Yuhan, C., Yu, X., & Mao, Z. (2024). Deep brain stimulation versus vagus nerve stimulation for the motor function of poststroke hemiplegia: Study protocol for a multicentre randomised controlled trial. BMJ Open, 14(10), e086098. https://doi.org/10.1136/bmjopen-2024-086098

Yamada, K., & Nabeshima, T. (2003). Brain-Derived neurotrophic factor/trkb signaling in memory processes. Journal of Pharmacological Sciences, 91(4), 267-270. https://doi.org/10.1254/jphs.91.267